Journal for ImmunoTherapy of Cancer

Chemical priming of natural killer cells with branched polyethylenimine for cancer immunotherapy

Seung Hee Choi ,[1] Hye Jin Kim,[1] Joo Dong Park ,[1] Eun-Su Ko ,[1] Minwook Lee ,[1] Dae-Keum Lee,[1] Jin-Ho Choi,[1] Hye Jung Jang,[1] Isaac Kim,[2] Hae-Yun Jung,[1] Keun-Hong Park ,[1] Kyung-Soon Park [1]

To cite: Choi SH, Kim HJ, Park JD, *et al*. Chemical priming of natural killer cells with branched polyethylenimine for cancer immunotherapy. *Journal for ImmunoTherapy of Cancer* 2022;**10**:e004964. doi:10.1136/jitc-2022-004964

► Additional supplemental material is published online only. To view, please visit the journal online (http://dx.doi.org/10.1136/jitc-2022-004964).

SHC and HJK contributed equally.

Accepted 24 July 2022

[1]Department of Biomedical Science, CHA University, Seongnam-si, Korea (the Republic of)
[2]Department of Surgery, Bundang CHA Medical Center, CHA University, Seongnam-si, Korea (the Republic of)

Correspondence to
Professor Keun-Hong Park; pkh0410@cha.ac.kr

Professor Kyung-Soon Park; kspark@cha.ac.kr

ABSTRACT

Background Due to their powerful immune surveillance activity and ability to kill and clear cancer cells, natural killer (NK) cells are an emerging anticancer immunotherapeutic agent. Therefore, there is much interest in developing efficient technologies that further enhance the therapeutic antitumor efficacy of NK cells.

Methods To produce chemically primed NK cells, we screened polymers with various electric charges and examined their ability to enhance the cytotoxicity of NK cells. The effect of primary amine and electric charges of 25 kDa branched polyethylenimine (25KbPEI) was investigated by fluorination of the chemical. The role of 25KbPEI in determining the major priming mechanism was investigated in terms of calcium influx into NK cells. In vivo therapeutic efficacy of chemically primed NK cells was evaluated against solid tumor mouse model of triple negative breast and ovarian cancers.

Results Chem_NK that was produced by the priming activity of 25KbPEI showed potent antitumor activity to various cancer cells. Chem_NK showed an activated phenotype, which manifests as increased expression of activating/adhesion/chemokine receptors and perforin accumulation, leading to enhanced migration ability and antitumor activity. Chem_NK display potent therapeutic efficacy against in vivo mouse model of triple negative breast and ovarian cancers. Fluorination of the primary amine group reduces the activity of 25KbPEI to prime NK cells, indicating that the cationic charge on the chemical plays a critical role in NK cell activation. A major priming mechanism was 25KbPEI-mediated calcium influx into NK cells, which occurred mainly via the $Ca2^{+}$-permeable non-selective cation channel transient receptor potential melastatin 2.

Conclusions NK cells can be chemically primed with 25KbPEI to express potent antitumor activity as well as enhanced migration ability. Because PEI is a biocompatible and Food and Drug Administration-approved chemical for biomedical use, these results suggest a cost-effective and simple method of producing therapeutic NK cells.

WHAT IS ALREADY KNOWN ON THIS TOPIC

⇒ Current technologies to enhance the therapeutic antitumor activity of natural killer (NK) cells are (1) genetic engineering to express chimeric receptor, and (2) priming with cytokine cocktail comprising interleukin-12/15/18.

WHAT THIS STUDY ADDS

⇒ NK cells can be chemically primed by 25 kDa branched polyethylenimine to display potent therapeutic efficacy against hard-to-treat solid cancers such as triple negative breast and ovarian cancers.

HOW THIS STUDY MIGHT AFFECT RESEARCH, PRACTICE OR POLICY

⇒ Chemical approaches to increase the antitumor activity of immune cells would facilitate development of the next generation of immune cell products with potent clinical activity.

BACKGROUND

Cationic polymers possess a unique structure that facilitates effective cellular uptake[1 2]; therefore, they are expected to have many applications in the field of pharmaceutical and medical sciences. Polyethylenimine (PEI) is a typical polycationic organic polymer with a high ionic charge density.[3 4] The structure of PEI is characterized by repeated amine groups sandwiched between two aliphatic carbon CH_2CH_2 spacers. Since cationic PEI binds to anionic cell membranes and enters cells via endocytosis, it is expected to have a variety of 'tunable' activities depending on its intracellular concentration. For example, the amine moieties of PEI can undergo protonation, which results in physiological damage via membrane depolarization and an increase in the intracellular pH.[5 6] PEI is available in a range of sizes and structures, including branched and linear forms of different molecular weight. Linear and branched PEI also differ with respect to amine groups: linear PEI contains only secondary amine groups, whereas branched PEI (bPEI) possesses primary, secondary, and tertiary amine groups.[7] Though the cationic properties of PEI are used routinely to generate nanoparticles for delivery of nucleic acids into the

cytoplasm of various cells, no study has asked whether PEI possess distinct biological activities, particularly toward immune cells.

Natural killer (NK) cells, cytotoxic lymphocytes within the innate immune system, are able to detect and lyse transformed or infected cells. Since NK cells from an allogeneic source can be administered safely to the recipient to target cancer cells in a non-major histocompatibility complex restricted manner, it is feasible to manufacture NK cells as 'off the shelf'-type therapeutics.[8 9] Accumulated evidence suggests that NK cells play a pivotal role in exerting robust antitumor responses and preventing metastasis of solid tumors.[10 11] The clear link between the number of tumor-infiltrating NK cells and activation of dendritic cells suggests that the antitumor activity of NK cells is not limited to innate immunity, but also operates in the adaptive arm.[12] A recent report demonstrates that NK cells engineered to express the anti-CD19 chimeric antigen receptor (CAR) and interleukin (IL)-15 show outstanding therapeutic efficacy against CD19-positive lymphoid tumors, without major toxic side effects.[13] In line with this successful translational application of CAR-NK cells to clinical platforms, there is much interest in developing efficient technologies that further enhance the therapeutic antitumor efficacy of NK cells. One of these technologies is a priming strategy that preactivates NK cells using a cytokine cocktail or leukemia cell lysate. A cytokine cocktail comprising IL-12/15/18 effectively primes mouse and human NK cells, resulting in augmented antitumor activity; in addition, leukemia cell lysates are sufficient to activate human NK cells in the absence of exogenous cytokines.[14 15] Although it is reported that a pharmacologic inhibitor of GSK3 kinase can be applied to NK cells as a supplement to cytokines to enhance their priming efficacy,[16] little research has been done to develop a chemical method of priming NK cells.

A previous study shows that the antitumor activity of NK cells is enhanced by cationic nanoparticles coated with 25 kDa bPEI (25KbPEI)[17]; therefore, we asked whether polymeric chemicals for nano-biotechnology applications have unidentified biological functions, especially with respect to immunity. Here, we screened polymers with various electric charges and examined their ability to enhance the cytotoxicity of NK cells. We found that 25KbPEI augments the anticancer activity of both primary NK cells and the NK92MI cell line. NK cells primed by 25KbPEI showed augmented antitumor activity in vitro and in vivo; such activities were mediated by increased expression of activating/adhesion/chemokine receptors and increased perforin accumulation, resulting in inhibition of tumor growth (even that of difficult-to-treat solid cancers). We also demonstrate that the cationic charge imparted by the primary amine of 25KbPEI is critical for priming activity, and for modulation of the intracellular cytoplasmic Ca^{2+} concentration $[Ca^{2+}]_i$.

METHODS

Cell lines

Human NK cell line (NK92MI) and human breast cancer cell lines (MDA-MB231, Hs578T, and MCF7) were purchased from the American Type Culture Collection (ATCC). Human gastric cancer cell lines (SNU484 and SNU638) were purchased from the Korean Cell Line Bank. Human ovarian cancer cell lines (A2780 and OVCAR3) were purchased from the ATCC.

NK92MI cells were cultured in Minimum Essential Medium-alpha, which is devoid of ribonucleosides and/or deoxyribonucleosides (Gibco/Life Technologies, GrandIsland, New York, USA) and supplemented with 2 mM L-glutamine (Gibco/Life Technologies), 0.2 mM inositol (Sigma-Aldrich, St. Louis, USA), 0.1 mM 2-mercaptoethanol (Gibco/Life Technologies), 0.02 mM folic acid (Sigma-Aldrich), 12.5% fetal bovine serum, and 1% penicillin/streptomycin (Gibco/Life Technologies). Cancer cells were grown in Dulbecco's Modified Eagle Medium or Roswell Park Memorial Institute 1640 medium (Gibco/Life Technologies) supplemented with 10% fetal bovine serum and 1% penicillin/streptomycin (Gibco/Life Technologies). All cultured cells were incubated at 37°C in a humidified incubator containing 5% CO_2

Primary NK cells

Human primary NK cells were purified from peripheral blood mononuclear cells, as described previously.[18] Primary NK cells were cultured in Advanced Roswell Park Memorial Institute 1640 medium with non-essential amino acids (Gibco/Life Technologies) supplemented with GlutaMAX-I Supplement (Gibco/Life Technologies), 10% fetal bovine serum, and 1% penicillin/streptomycin (Gibco/Life Technologies). Primary NK cells were cultured in the presence of fresh recombinant human IL-2 (10 ng/mL; PeproTech) and IL-15 (5 ng/mL; PeproTech) for 14 days.

Generation of Chem_NK

Chem_NK was generated by treating NK92MI cells with a 25KbPEI (408727, Sigma-Aldrich). A stock solution of 25KbPEI (10 mg/mL) was prepared by dilution in DW (purified water) and added to the culture medium of NK cells (1×10^6 cells/9.6 cm^2) to yield a final concentration of 5 µg/mL. The surface membrane of Chem_NK was observed under a Scanning Electron Microscope (S-3000N, Hitachi, Japan). Intracellular localization of 25KbPEI in Chem_NK was observed using an FV3000 confocal microscope (Olympus).

Synthesis and characterization of fbPEI

25KbPEI (10 mg) was dissolved in methanol, followed by addition of 2 mL of heptafluorobutyric anhydride (H1006, Sigma-Aldrich). The mixture was stirred at room temperature for 24 hours and then dialyzed for 2 days against distilled water at room temperature (molecular weight cut-off 2K). The distilled water was

replaced every 2 hours (dialysis overnight was carried out without replacing the distilled water). The product was lyophilized to obtain fluorinated bPEI (fbPEI) as a white gel. It was then dissolved in distilled water and used for the experiments. The zeta potential of bPEI and fbPEI was measured by dynamic light scattering (Zetasizer Nano ZS, Malvern Panalytical, Malvern, UK). Gel retardation assays were performed to analyze DNA binding affinity. bPEI and fbPEI (3.5, 7, 10.5, 17.5, and 24.5 µg) were combined with 20 µg of plasmid DNA, followed by electrophoresis. DNA band volume was analyzed quantitatively. bPEI and fluorinated PEI were dissolved in D_2O and analyzed by 500 MHz liquid NMR (Bruker, Massachusetts, USA) at the Korea Basic Science Research Institute.

Cytotoxicity assay of NK cells

Target (cancer) cells were pre-stained with 1 µM of Cell Trace CFSE (Invitrogen) to sort target cells by flow cytometry. Then, stained target cells were co-cultured with effector (NK) cells at the E:T (effector:target) ratio indicated in the figure legends. After 4 hours, whole cells were harvested and stained with 7-AAD (Invitrogen) to differentiate live and dead cells, and then fixed with 2% paraformaldehyde. Target cell lysis is expressed as the percentage of $CFSE^{+}$7-AAD^{+} cells. Cells were detected using a CytoFLEX flow cytometer (Beckman Coulter) and data were analyzed using FlowJo software (Tree Star Inc.).

Degranulation assay

To measure the degranulation of NK cells, NK92MI cells were co-cultured with green fluorescent protein (GFP) expressing MDA-MB231 cells for 4 hours at an E:T ratio of 0.5:1. Co-cultured cells were stained with APC anti-human CD107a (BD Biosciences, San Jose, California, USA) for 30 min at 4°C and then analyzed using a CytoFLEX flow cytometry.

Time-lapse observation of NK cell activity

GFP-expressing MDA-MB231 cells (1×10^4 cells) were seeded into a culture plate and co-cultured with NK92MI cells (ratio, 1:1) in an Olympus FV3000 incubation system. The time taken for NK cells, which were stained with CellTrace Far Red (C34572, Invitrogen), to bind to MDA-MB231 cells was evaluated by examining the movement of a single NK cell under a time-lapse microscope. A dead cell indicator (7-AAD) was added to the culture medium and time lapse imaging was performed every 3 min for 10 hours. The killing efficiency of Chem_NK was evaluated by real-time imaging. A modified Olympus FV3000 microscope fitted with a 60X (UIPlanXApo, NA=1.42, oil immersion) objective lens was used for the imaging experiments. The focus of the confocal microscope was controlled automatically by a Z drift compensation system. Acquired image data were analyzed using cellSens software (Olympus).

Time-lapse observation of 25KbPEI-mediated calcium influx into NK cells

25KbPEI-mediated influx of calcium into NK92MI was observed using the calcium-sensitive fluorochrome Fluo-4-AM (Thermo Fisher Scientific). Briefly, the culture medium of NK92MI cells was spiked with 25KbPEI and Fluo-4-AM, and confocal live imaging of calcium influx was performed using an FV3000 confocal microscope (Olympus, Tokyo, Japan) equipped with INCUBATOR T (Live Cell Instruments, Seoul, Korea); measurements were taken every 1 min for up to 30 min. To analyze the effects of calcium influx on 25KbPEI-mediated perforin accumulation, NK92MI cells were preincubated in Ca^{2+}-free suspension minimum essential medium media (SMEM,Gibco) for 30 min at 37°C. Then, 25KbPEI was added along with Fluo-4-AM. Imaging of calcium influx, represented by Fluo-4-AM fluorescence, was performed using an FV3000 confocal microscope (Olympus). The fluorescence intensity of Flou-4 AM was quantified by flow cytometry.

Quantitative RT-PCR

Total RNA was prepared using TRIzol reagent (Invitrogen, Carlsbad, California, USA) and complementary DNA was synthesized from 1 µg of total RNA using the SuperScript II First-Strand Synthesis System (Invitrogen). Quantitative real-time PCR (qRT-PCR) was performed using iQ SYBR Green PCR Master mix (Bio-Rad, Hercules, California, USA) and the CFX Connect Real-Time PCR Detection System (Bio-Rad). *GAPDH* was used as an internal control to normalize the qRT-PCR data. The qRT-PCR was performed using the following primers: *perforin*, Forward, gggattccagagcccaagtg and Reverse, gagaaggatgcccaggagga; *granzyme B*, Forward, tgcaggaagatcgaaagtgcg and Reverse, gaggcatgccattgtttcgtc; and *GAPDH*, Forward, acccacagtccatgccatcac and Reverse, tccaccaccctgttgctgta.

Immunoblot analysis

For immunoblotting, NK92MI cells were lysed with cell lysis buffer (Cell Signaling Technology, Danvers, Massachusetts, USA) containing protease inhibitors and phosphatase inhibitors (Thermo Fisher Scientific, Waltham, Massachusetts, USA). Cell lysates were separated by sodium dodecyl sulfate-polyacrylamide gel electrophoresis and transferred to polyvinylidene difluoride membranes (Bio-Rad). Membranes were blotted with anti-perforin (Abcam, Zotal, Israel), anti-granzyme B (Abcam), and anti-GAPDH (Cell Signaling Technology) antibodies.

Migration assay

Migration of NK92MI to target cells was analyzed using a 24 well-insert Transwell chamber (8.0 µm, Falcon). Briefly, 5×10^5 NK92MI pre-stained with 1 µM CellTrace CFSE (Invitrogen) in serum-free medium were loaded on the Transwell insert. Next, 5×10^5 target cancer cells in complete medium were seeded into the bottom

chamber. After incubation for 12 hours, migrated NK92MI cells were counted using LUNA cell counter (Logos).

Flow cytometry analysis

NK cells were washed with FACS buffer (BD Biosciences, San Jose, California, USA) and blocked with Fc blocker (BD Biosciences) for 15 min at room temperature. After incubation for 30 min at room temperature with a fluorochrome-conjugated antibody, antibody-labeled NK cells were fixed for 15 min with 1% paraformaldehyde. Flow cytometry analysis was performed using a CytoFLEX flow cytometer (Beckman Coulter). Data were analyzed using FlowJo software (Tree Star). The isotype controls and antibodies used in these studies are listed in online supplemental table S1.

In vivo animal experiments

MDA-MB231 xenograft tumors were established in 6-week-old (17–20 g) female nude/SCID mice (JAbio, South Korea). Briefly, 5×10^6 MDA-MB231 cells, engineered to express GFP and luciferase, were injected orthotopically into the mammary fat pad. Tumor size was estimated by luciferase imaging using a Pearl Impulse (LI-COR Biosciences). Tumor volume was calculated using the following formula: volume = $(\text{width}^2 \times \text{length})/2$. Starting at 13 days post-tumor cell transplantation, 1×10^7 NK cells were injected intratumorally two times per week for 4 weeks.

A2780 xenograft tumors were established in 6-week-old (17–20 g) female NSGA mice (SCID-mediated total Immune Deficient mice) (JAbio, South Korea). Briefly, 5×10^5 cancer cells engineered to express GFP and luciferase were injected intraperitoneally into mice. Intravenous injection of 1×10^7 NK cells were performed two times per week for 4 weeks, starting form 4 days after tumor injection.

To measure luciferase intensity, mice were injected intraperitoneally with 4 mg/kg of Luciferin (Promega). After 10 min, mice were anesthetized with 2% isoflurane for 10 s and then imaged using the Pearl Impulse Small Animal Imaging System (LI-COR Biosciences) and Image Studio V.5.2 software. Mice were housed in a semi-specific pathogen-free animal facility at CHA University (Seongnam, Korea). All animal experiments were approved by the Institutional Animal Care and Use Committee (IACUC 200011, IACUC 210026) of CHA University and were carried out in accordance with approved protocols.

Statistical analysis

GraphPad Prism V.9.0 software (GraphPad Software, La Jolla, California, USA) was used for all statistical analyses. The details of the statistical tests conducted are indicated in the figure legends. Statistical significance is reported as follows: NS, not significant; *p<0.05; **p<0.01; ***p<0.001 or ****p<0.0001

RESULTS

25KbPEI primes NK cells to enhance anticancer cytotoxicity

We screened chemicals used widely in nanobiotechnology to identify those prime NK cells. We selected 13 chemicals with various electric charges at pH 7.5. To examine the effects of these chemicals on the cytotoxicity of NK cells, we first determined the concentration of each chemical that maintained the viability of NK92MI cells at more than 80% (online supplemental figure 1). The different chemicals were added to the culture medium of NK92MI cells for 24 hours. When the cytotoxicity of NK cells was tested against MDA-MB231 (a triple negative breast cancer cell line) in a CFSE-7-AAD assay, we found that activity of NK92MI cells incubated with bPEI with a molecular weight of 25 kDa or 70 kDa (25KbPEI or 70KbPEI, respectively) was more than twofold than that of non-primed control NK cells (figure 1A, online supplemental figure 2). Time course analysis of the effect of 25KbPEI on NK92MI cells revealed that the ability to increase cytotoxicity peaked at 12 hours post-treatment (online supplemental figure 3). Since the ability of 25KbPEI and 70KbPEI to increase NK92MI cytotoxicity was similar, we named NK92MI cells treated with 25KbPEI for 12 hours as Chem_NK and used them for all further experiments. The proliferation of Chem_NK was comparable to that of C_NK (data not shown). Chem_NK showed 25% cytotoxicity against MDA-MB231 at an effector:target cell (E:T) ratio of 1.25:1, whereas the cytotoxicity of control NK92MI (C_NK) was approximately 20% at an E:T ratio of 10:1 (figure 1B); overall, the cytotoxicity data suggest that Chem_NK are more cytotoxic to MDA-MB231 cells than C_NK, even at one-tenth the cell number. Consistently, a significant increase in CD107a expression was observed in Chem_NK compared with C_NK in the presence of target cells (figure 1C). Moreover, Chem_NK secreted a greater quantity of interferon-gamma than C_NK both in the presence and absence of target cells (data not shown). Chem_NK showed enhanced cytotoxic activity against six additional cancer cell lines: breast cancer lines Hs578T and MCF7; gastric cancers lines SNU484 and SNU638; and ovarian cancer lines A2780 and OVCAR3. This indicates augmented Chem_NK activity against a broad spectrum of cancers (figure 1D). Currently, primary NK (pNK) cells purified from various sources (including peripheral blood from healthy donors) and expanded with various cytokine cocktails are being evaluated clinically for their antitumor efficacy.[19] Notably, IL-2, IL-12, IL-15, and IL-18, which are typically used to prime pNK cells cultured ex vivo,[20–22] did not limit 25KbPEI's capacity to enhance the anticancer activity of human peripheral blood-derived pNK cells (online supplemental figure 4). Similar to NK92MI cells, pNK cells primed by 25KbPEI showed significantly enhanced cytotoxic activity against all cancer cell lines, but not against fibroblasts, suggesting that chemically primed

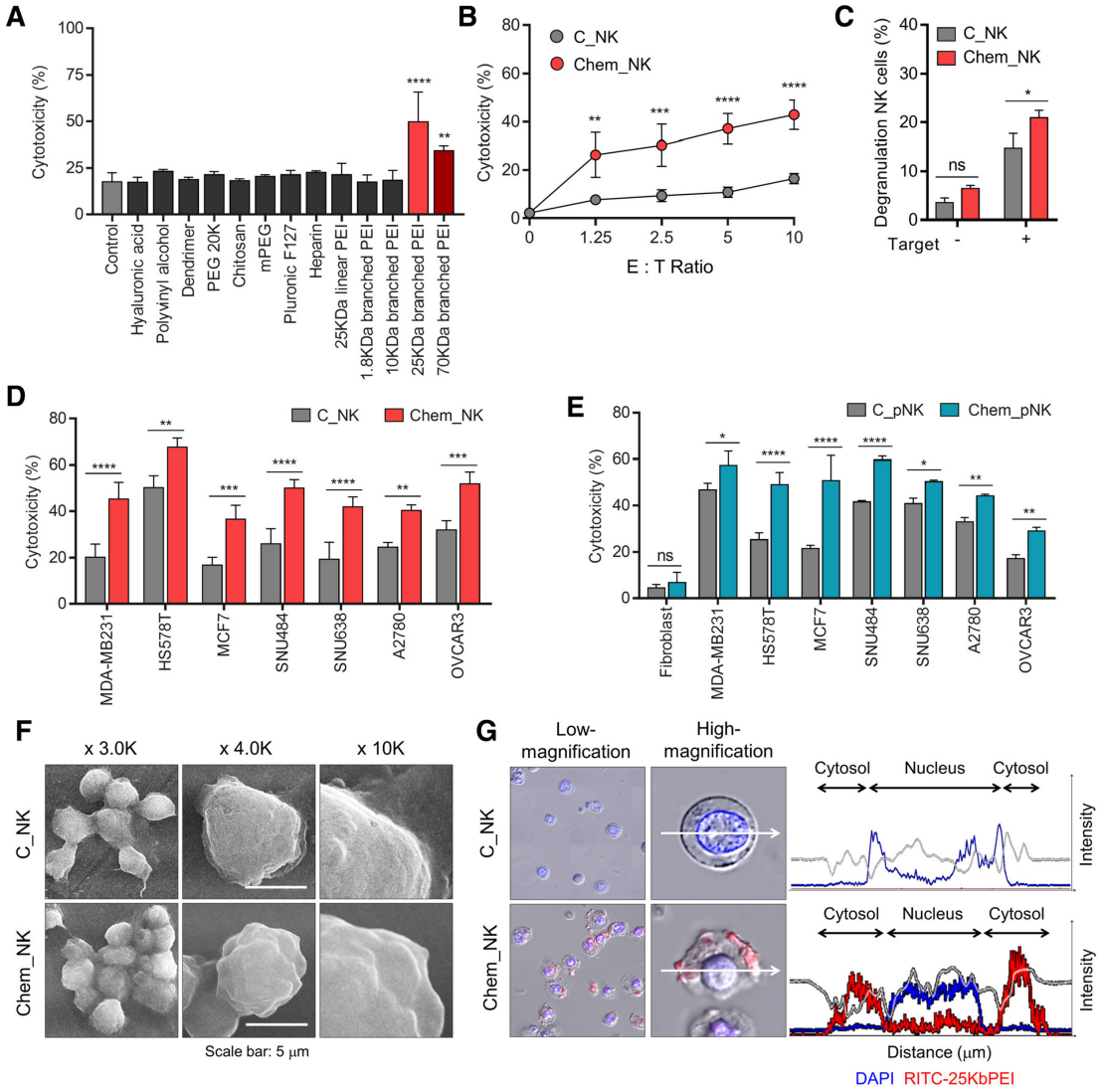

Figure 1 25KbPEI primes NK cells to enhance cytotoxicity against cancer cells. (A) A CFSE-7-AAD assay to measure the cytotoxic activity of NK92MI cells treated with the indicated chemicals. The target cells were MDA-MB231, and the E:T ratio was 10:1. Statistical significance was evaluated using one-way ANOVA with Dunnett's multiple comparisons test. (B) The cytotoxicity of control (C_NK) or 25KbPEI-treated NK92MI (Chem_NK) was analyzed at the indicated E:T ratios was measured in a CFSE-7-AAD assay. (C) The cytotoxicity of control (C_NK) or 25KbPEI-treated NK92MI (Chem_NK) was measured in a CD107a assay at an E:T ratio 1:1. (D) The cytotoxicity of C_NK and Chem_NK against the indicated cancer cells was analyzed in a CFSE-7-AAD assay at an E:T ratio 10:1. (E) The cytotoxicity of control (C_pNK) and 25KbPEI-treated primary NK cells (Chem_pNK) against the indicated cells was analyzed in an CFSE-7-AAD assay at an E:T ratio 10:1. (F) Cell morphology of C_NK and Chem_NK was observed under a scanning electron microscope. (G) Image of RITC-labeled 25KbPEI localized in the cytoplasm of NK92MI. NK92MI cells were treated with RITC-labeled 25KbPEI for 12 hours. All analyzes were performed at least in triplicate. Data represent the mean±SD of three independent experiments. Statistical comparisons were conducted using two-way ANOVA with Sidak's multiple comparisons tests. *p<0.05, **p<0.01, ***p<0.001, ****p<0.0001. ANOVA, analysis of variance; E:T, effector:target; NK, natural killer; PEI, polyethylenimine; 25KbPEI, 25 kDa branched PEI.

pNK cells maintain their ability to distinguish target cells from non-target cells (figure 1E).

Human peripheral blood-derived pNK cells are typically divided into two subsets, $CD56^{bright}$ and $CD56^{dim}$,[23] with immature ($NKG2A^{+}KIR^{+}CD57^{-}$) and mature ($NKG2A^{-}KIR^{+}CD57^{+}$) populations comprising $CD56^{dim}$ populations.[24] The priming activity of 25KbKPEI was effective on both $CD56^{bright}$ and $CD56^{dim}$ pNK cells (online supplemental figure 5a), and immature $CD56^{dim}$ ($NKG2A^{+}KIR^{+}CD57^{-}$) responded more effectively to 25KbPEI than mature $CD56^{dim}$ ($NKG2A^{-}KIR^{+}CD57^{+}$) populations (online supplemental figure 5b).

The phenotype of Chem_NK led to rapid aggregation; indeed, most RITC-labeled 25KbPEI was detected in the cytoplasm of NK92MI at 12 hours post-incubation (figure 1F,G), indicating that 25KbPEI exerted its activity after internalization into NK cells. Based on these results, we conclude that NK cells can be chemically primed by 25KbPEI.

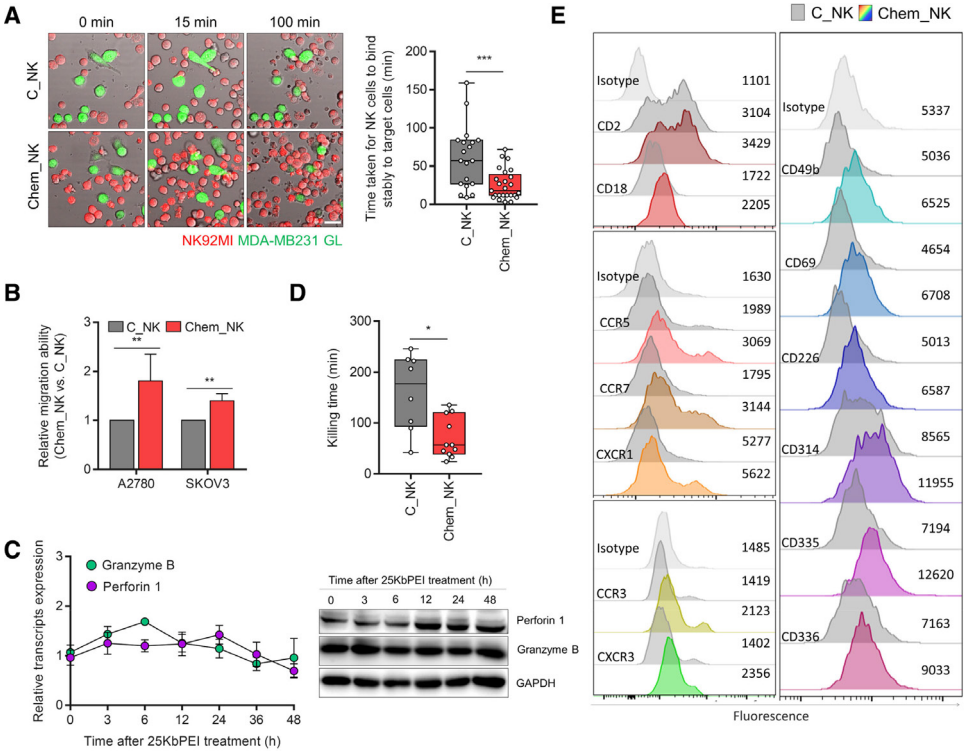

Figure 2 Phenotypic properties of Chem_NK associated with antitumor activity. (A) Images showing apoptosis of target cells (green fluorescent protein-expressing MDA-MB231 (MDA-MB231 GL)) co-incubated with far red-stained C_NK or Chem_NK for the indicated times. Scale bars, 30 µm (left panel). Time taken for C_NK or Chem_NK cells to bind stably to target cells (right panel). NK cells that bound to target cells for longer than 3 min were regarded as making 'stable' contact. (B) Quantitative analysis C_NK and Chem_NK migration toward two ovarian cancer cell lines, A2780 and SKOV3, in a Transwell assay. Statistical comparisons were conducted using the Mann-Whitney U test. (C) Expression of perforin 1 and granzyme B following 25KbPEI treatment for the indicated times was evaluated by quantitative real-time PCR and immunoblot analysis. (D) Time taken for C_NK and Chem_NK cells to induce lysis of MDA-MB231 cells after making stable contact. (E) Flow cytometry analysis of expression of the indicated receptors on C_NK and Chem_NK cells. Data are presented as the mean±SD of more than three independent experiments. *p<0.05, **p<0.01, ***p<0.001. NK, natural killer; 25KbPEI, 25 kDa branched polyethylenimine.

Chem_NK cells show a phenotype suggestive of enhanced cytotoxicity

To determine the primary effector mechanisms underlying the anticancer cytotoxicity of Chem_NK, we examined the interaction between Chem_NK and MDA-MB231 cells using time-lapse microscopy. We found that a large number of Chem_NK migrated toward cancer cells, whereas non-primed C_NK randomly bumped into target cells (figure 2A, left panel). The phenotype of Chem_NK was assessed by measuring the time taken for NK cells to make stable contact (contact duration >3 min) with a target cell. Consistent with the microscopic observations, time to make stable contact with MDA-MB231 cells was significantly shorter for Chem_NK cells than for C_NK cells (figure 2A, right panel). An in vitro transwell assay with ovarian cancer cell lines A2780 and SKOV3 confirmed that Chem_NK migrated to target cells more efficiently than C_NK (figure 2B). On recognition of and binding to cancer cells, NK cells release the contents of cytolytic granules; pore-forming perforin and the serine protease granzyme.[25] To confirm whether Chem_NK also had an increased capacity to induce apoptosis, we examined the effects of 25KbPEI on granzyme and perforin levels. Compared with C_NK cells, the amount of perforin in Chem_NK was significantly higher at 12 hours post-stimulation with 25KbPEI, even though transcription of the respective genes was unchanged (figure 2C and online supplemental figure 6a). The accumulation of perforin protein was also observed in human pNK cells on exposure to 25KbPEI (online supplemental figure 6b).

Consistent with this, the time taken for NK cells to induce apoptosis after making stable contact (contact duration >3 min) with target cells was markedly shorter for Chem_NK than for C_NK (figure 2D).

Chem_NK had higher expression levels of activating, cell-to-cell adhesion and inhibitory receptors than C_NK (figure 2E and online supplemental figure 7). Given that cytolytic activity of NK cells is governed by a repertoire of receptors, 25KbPEI-mediated alteration in receptors of NK cells may have shifted the activity balance toward NK cell activation.

Collectively, we concluded that 25KbPEI effectively primes NK cells to exert potent antitumor activity.

In vivo antitumor activity of Chem_NKs toward hard-to-treat solid tumors

Given that Chem_NK cells show enhanced migration toward ovarian cancer cells in vitro (figure 2C), we

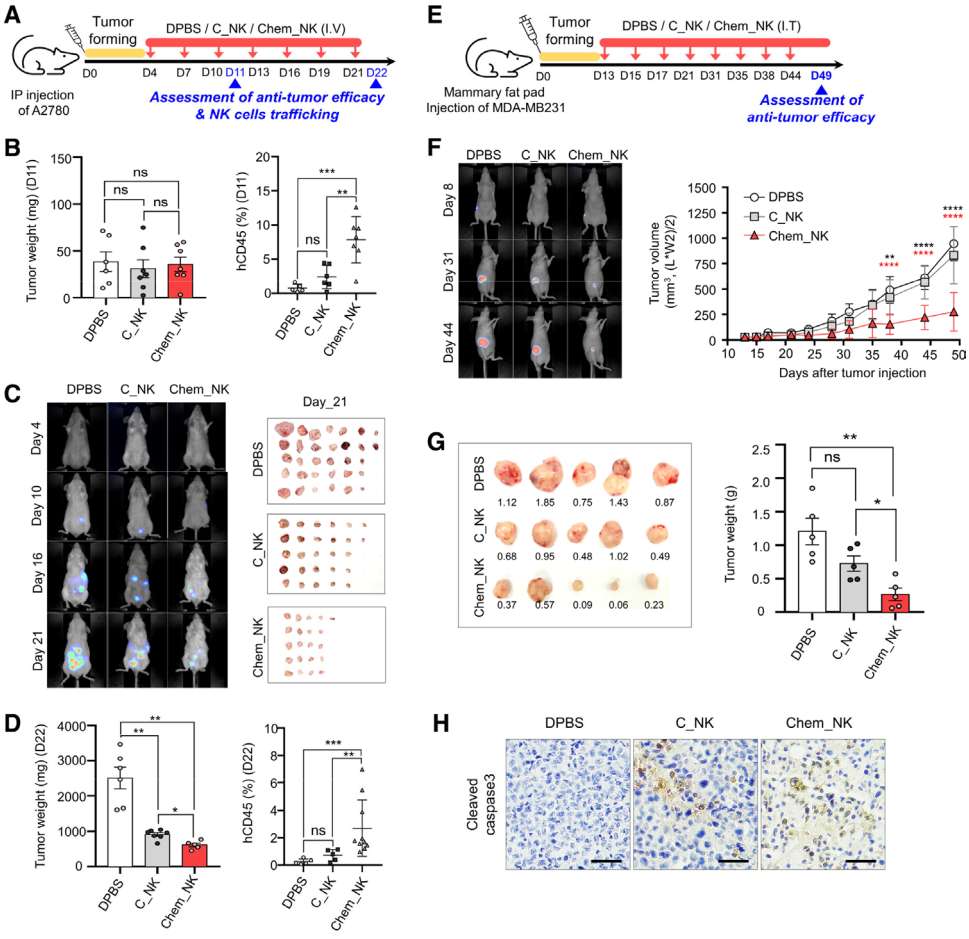

Figure 3 Antitumor activity of Chem_NK against hard-to-treat solid tumors in vivo. (A) The A2780 xenograft mouse model used to study the in vivo antitumor efficacy of NK cells (each group n=5). (B) Average tumor weight and the amount of infiltrating CD45$^+$ NK cells present in each tumor in the indicated mouse group were analyzed at 11 days post-tumor implantation. (C) Luminescence images of A2780 tumor-bearing NSG mice following intravenous injection of C_NK, Chem_NK cells or DPBS (control) on the indicated days (left panel). Resected tumors were harvested at 26 days post-tumor implantation (right panel). (D) Average tumor weight and the amount of infiltrating CD45$^+$ NK cells present in each tumor from the indicated mouse group were analyzed at 26 days post-tumor implantation. (E) MDA-MB231 orthotopic mouse model used to study the in vivo antitumor efficacy of NK cells (each group n=5). (F) Luminescence images of MDA-MB231 tumor-bearing nude mice following intratumoral injection of C_NK, Chem_NK, or DPBS on the indicated days (left panel). Average tumor growth in each mouse group (right panel). (G) Image of resected tumors (left panel) and average tumor weight (right panel); tumors were harvested at 49 days post-implantation (left panel). (H) Immuno-histochemical staining for cleaved caspase-3 in the indicated tumor sections. Data represent the mean±SD of three independent individuals. Statistical comparisons were conducted using two-way analysis of variance with Sidak's multiple comparisons tests. *p<0.05, **p<0.01, ***p<0.001, ****p<0.0001. IP, intraperitoneal; NK, natural killer.

examined their in vivo trafficking ability and antitumor efficacy. To do this, we used a xenograft (A2780) NSG mouse model of ovarian cancer. NK cells were administered intravenously into mice seven times every 3 days, as indicated in figure 3A. Consistent with in vitro results, Chem_NK infiltration into 11-day-old tumors was greater than that of C_NK, even though there was no difference in tumor weight between the groups on the examined day (figure 3B). After seven doses of NK cells, the tumor burden in the Chem_NK group was lower than that in the control group, and the number of intratumoral NK cells was higher in the Chem_NK group (figure 3C,D and online supplemental figure 8). The antitumor activity of Chem_NK was further evaluated in a xenograft model of triple negative breast cancer (MDA-MB231) (figure 3E). As expected, tumors in the Chem_NK group were significantly smaller than those in the DPBS group and C_NK groups (figure 3F,G and online supplemental figure 9). Immunohistochemical staining of tumor sections showed that tumors from the Chem_NK group contained more cleaved caspase-3 than those from the C_NK group, indicating that Chem_NK induced apoptosis of target tumor cells to a greater extent than C_NK (figure 3H). Taken together, these in vivo data demonstrate that Chem_NK have potent antitumor efficacy against hard-to-treat solid tumors such as ovarian and breast cancers.

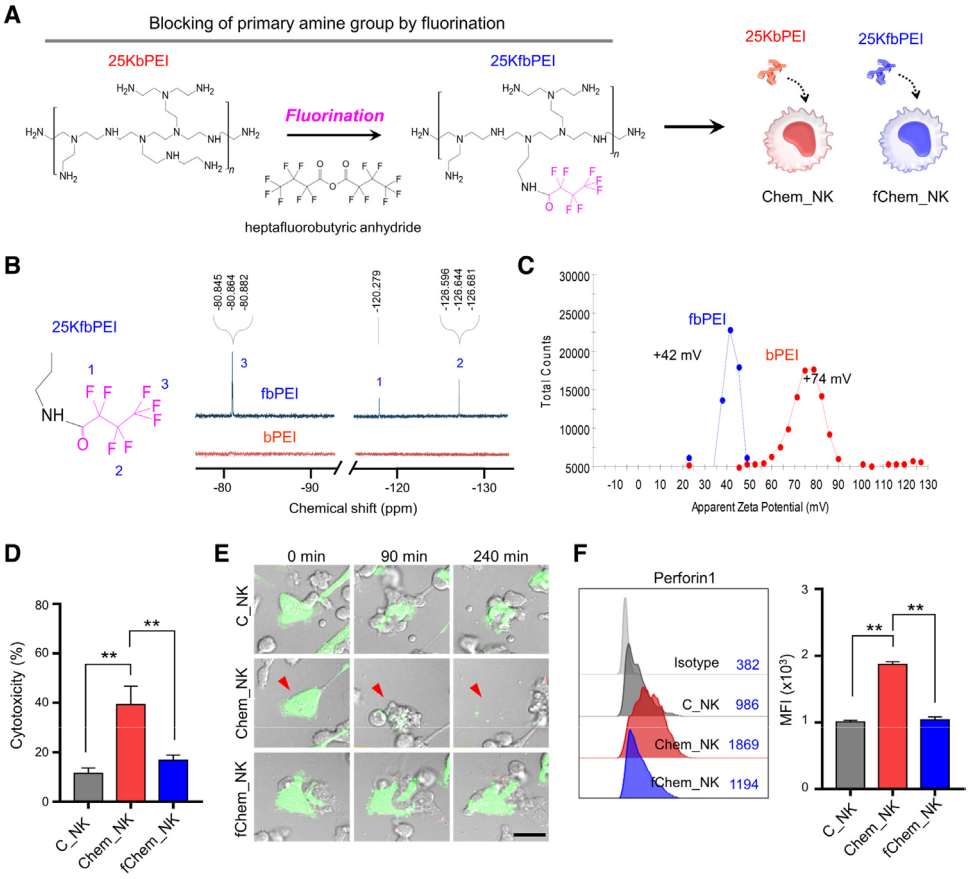

Figure 4 Priming activity of 25KbPEI depends on the cationic charge of the chemical. (A) Diagram showing fluorination of the primary amine group of 25KbPEI to generate 25KfbPEI, and the subsequent experimental process. (B) ^{19}F-NMR analysis of 25KbPEI and 25KfbPEI. Fluorocarbon peaks are labeled 1–3. (C) Measurement of the zeta potential of 25KbPEI and 25KfbPEI by dynamic light scattering. (D) The cytotoxicity of C_NK, Chem_NK, and fChem_NK (NK92MI cells treated with 25KfbPEI) against MDA-MB231 was analyzed in a CFSE-7-AAD assay at an E:T ratio 10:1. (E) Images showing apoptosis of target cells (green fluorescent protein-expressing MDA-MB231) co-incubated with C_NK, Chem_NK, or fChem_NK for the indicated times. Scale bars: 20 µm. (F) Flow cytometry analysis of perforin levels in C_NK, Chem_NK, and fChem_NK. All analyzes were performed at least in triplicate. Data represent the mean±SD of three independent experiments. Statistical significance was evaluated using one-way analysis of variance with Dunnett's multiple comparisons test; *p<0.05, **p<0.01. ***p<0.001. bPEI, branched PEI; fbPEI, fluorinated bPEI; E:T, effector:target; NK, natural killer; PEI, polyethylenimine; 25KbPEI, 25 kDa bPEI; 25KfbPEI, 25 kDa fbPEI.

The priming activity of 25KbPEI depends on its cationic charge

Given that linear form of PEI did not stimulate NK cells, we wondered whether the total number of primary amine groups in 25KbPEI is critical for NK cell-mediated cytotoxicity. To test this, we examined the effect of fluorination of the primary amine group of 25KbPEI (25KfbPEI) on its priming activity (figure 4A). The ^{19}F-NMR analysis revealed that peaks 1, 2, and 3 were present in 25KfbPEI, but not in 25KbPEI (figure 4B), indicating that the primary amine groups of 25KbPEI were fluorinated successfully. The ^{13}C-NMR analysis confirmed that the primary amine peak in the vicinity of 40 ppm decreased in 25KfbPEI, and that fluorocarbon (CF_2 and CF_3) peaks appeared between 110 and 120 ppm (online supplemental figure 10). The zeta potential of 25KfbPEI was significantly lower (by approximately 40%; +42 mV vs +74 mV) than that of 25KbPEI (figure 4C), suggesting that the cationic charge of 25KbPEI decreased after fluorination. Consistent with the zeta potential data, gel retardation assays revealed that the binding affinity of 25KfbPEI for plasmid DNA was lower than that of 25KbPEI (online supplemental figure 11).

When the priming activity of 25KfbPEI was examined in NK92MI cells, the cytotoxicity of 25KfbPEI-treated NK92MI cells (fChem_NK) was much lower than that of Chem_NK (figure 4D). The loss of priming activity of 25KfbPEI was further confirmed by time-lapse observations. As shown in figure 4E and online supplemental video 1, the cytotoxic activity of fChem_NK was similar to that of C_NK, both of which were much lower than Chem_NK. Consistent with this phenotype, 25KfbPEI did not induce perforin accumulation in NK92MI cells (figure 4F). These results suggest that blocking the primary amine in 25KbPEI results in extinction of NK stimulating activity. Thus, the ability of 25KbPEI to prime NK cells is attributable mainly to the activity of its primary amine group.

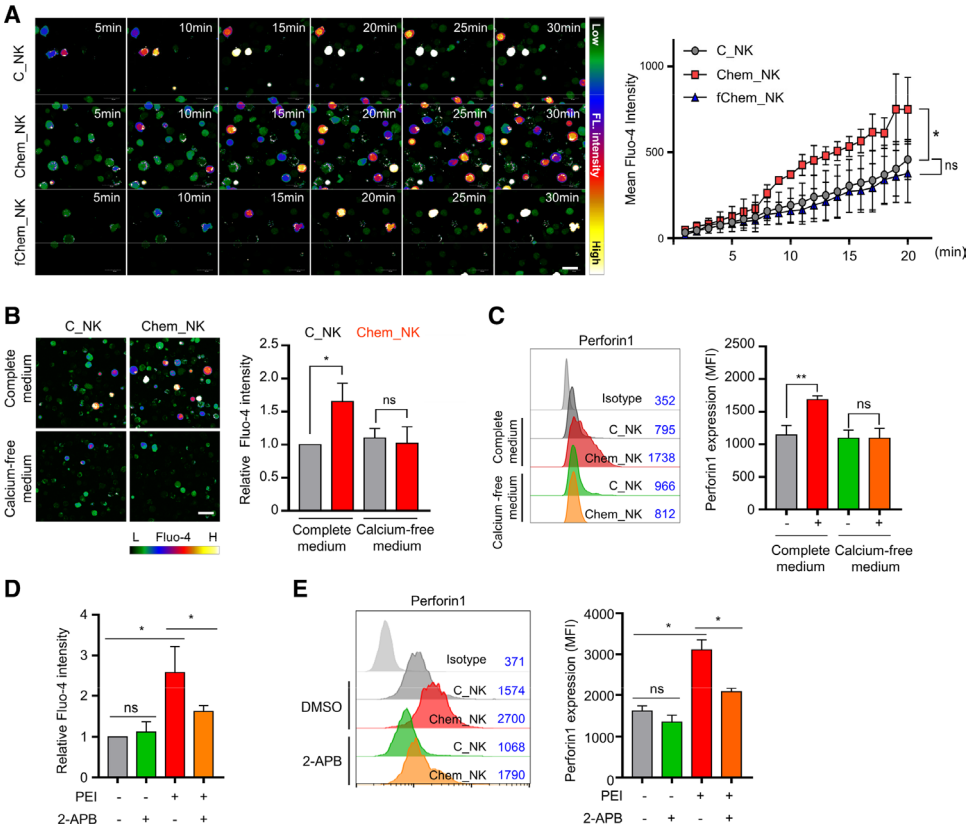

Figure 5 25KbPEI primes NK cells by inducing calcium influx. (A) Time-lapse microscopic observation of intracellular calcium influx, detected using the fluorescent calcium indicator Fluo-4 (left panel). Fluo-4 was added to the culture medium of C_NK cells containing 25KbPEI or 25KbfPEI, and calcium influx was monitored at the indicated times. The number of fluorescent (+) cells at the indicated times was counted (right panel). (B) Microscopic observation of the effect of 25KbPEI on intracellular calcium concentrations in C_NK cells cultured in complete or calcium-free medium. C_NK cells were cultured in the indicated culture media for 12 hours, followed by addition of 25KbPEI and Fluo-4 to monitor the effects of 25KbPEI on calcium influx (left panel). Flow cytometry-based quantitative analysis of NK cells containing fluorescent Fluo-4 (right panel). (C) Quantitative flow cytometry analysis of perforin protein levels in C_NK and Chem_NK cells cultured in complete medium or calcium-free medium. C_NK cells were cultured in the indicated media for 12 hours, followed by culture in the presence or absence of 25KbPEI for an additional 12 hours. Perforin levels were measured by flow cytometry analysis. (D) Flow cytometry-based quantitative analysis of C_NK or Chem_NK cells containing fluorescent Fluo-4 in the presence or absence of the transient receptor potential melastatin 2 inhibitor 2-aminoethoxydiphenyl borate (2-APB). (E) Quantitative flow cytometry analysis of perforin protein levels in C_NK and Chem_NK cells in the presence or absence of 2-APB. Data are representative of more than three independent experiments and values are expressed as the mean±SD. *p<0.05, **p<0.01; unpaired Student's t-test. NK, natural killer; PEI, polyethylenimine; 25KbPEI, 25 kDa branched PEI.

25KbPEI primes NK cells by inducing calcium influx

Next, we examined the mechanism underlying the ability of 25KbPEI to prime NK cells. Previous studies show that the cytoplasmic concentration of free Ca^{2+} ($[Ca^{2+}]_i$) is associated with the cargo of cytolytic granules. Specifically, $[Ca^{2+}]_i$ is closely related to perforin proteostasis (eg, proper folding in the endoplasmic reticulum (ER), and trafficking from the Golgi to cytosolic vesicles) in cytolytic lymphocytes.[26] Since 25KbPEI induces perforin accumulation without transcriptional activation (figure 2C), we questioned whether this phenotype in NK cells was caused by 25KbPEI-mediated perturbation of $[Ca^{2+}]_i$. As expected, a time-lapse experiment monitoring calcium concentrations in the cytoplasm of both NK92MI and primary NK cells clearly showed a rapid increase in $[Ca^{2+}]_i$ after treatment of 25KbPEI, but not after treatment with 25KfbPEI (figure 5A, online supplemental figure 12, online supplemental video 2). When 25KbPEI was added to NK92MI cultured in calcium-free medium, it did not induce perforin accumulation in NK cells (figure 5B,C), indicating that 25KbPEI-mediated increases in $[Ca^{2+}]_i$ are linked directly to accumulation of perforin in NK cells. Based on the finding that transient receptor potential melastatin 2 (TRPM2)-mediated Ca^{2+} signaling is involved in the antitumor activity of NK cells,[27 28] we examined the effect of 2-aminoethoxydiphenyl borate (2-APB), which inhibits the Ca^{2+}-permeable channel gating function of TRPM2, on the ability of 25KbPEI to enhance NK cell activity. As shown in figure 5D,E, 25KbPEI-mediated calcium influx and perforin accumulation was reduced significantly in the presence of 2-APB. Consistently, 2-APB inhibited the ability of 25KbPEI to induce calcium influx and perforin accumulation in human pNK cells (online supplemental figure 13). These results indicate

that TRPM2 is the main, but not exclusive, contributor to 25KbPEI-mediated calcium influx in NK cells.

DISCUSSION AND CONCLUSION

In summary, we propose a simple, economical, and potent strategy for increasing the antitumor activity of NK cells using 25KbPEI. Since 25KbPEI arms NK cells by increasing expression of activating/adhesion/chemokine receptor expression and perforin accumulation, the chemical instills a 'ready to fight' state in NK cells prior to target cell recognition. By fluorinating the primary amine groups of 25KbPEI, we demonstrated that these amine groups play a critical role in the priming activity of the chemical. Though we cannot rule out the possibility that there are multiple mechanisms by which 25KbPEI increases NK cell activity, our results suggest that 25KbPEI-mediated calcium influx is a major trigger that primes NK cells.

Along with serine protease granzymes, the pore-forming protein perforin is a representative cytotoxic cargo carried by cytotoxic lymphocytes, including NK cells. Following target cell recognition and microtubule-organizing center polymerization, perforin is oligomerized to form membrane-spanning pores that transfer granzymes from effector lymphocytes to target cells.[29] Compared with that of granzymes, the intracellular trafficking and safe storage of which are well understood,[30 31] our knowledge about the mechanism(s) underlying proteostasis of perforin is very limited. Perforin is synthesized as a 70 kDa monomeric precursor in the ER, and binding of Ca^{2+} to perforin is required for stable folding in the ER and subsequent trafficking to the cytoplasm, indicating that $[Ca^{2+}]_i$ is associated with perforin proteostasis in cytolytic lymphocytes.[26] Consistent with these reports, our data show that 25KbPEI-mediated calcium influx leads to accumulation of perforin.

By analyzing the effect of chemical inhibitors of various calcium channels on the effects of 25KbPEI in NK cells, we identified TRPM2 as a major channel involved in 25KbPEI-mediated calcium influx. Unlike TRPM2, chemical inhibition of voltage-dependent calcium channels could not block the ability of 25KbPEI to induce calcium influx (data not shown). Considering that 2-APB did not inhibit 25KbPEI-mediated calcium influx in NK cells completely, there might be unidentified other calcium channels involved in 25KbPEI activity. In addition, it is worthwhile to further study how 25KbPEI-mediated calcium influx induces perforin accumulation in NK cells.

We speculate that there are several unique advantages to application of Chem_NK in a clinical setting. First, Chem_NK represents an easy, fast, and economical method of generating anticancer NK cells. The high cost of lentivirus production and low efficiency of transduction into NK cells is a major obstacle to application of molecular engineering to production of CAR_NK cells.[32 33] Our study demonstrated that application of 25KbPEI as a component of the culture medium increased the antitumor activity of NK cells quickly and easily.

Second, considering that 25KbPEI increases the antitumor activity of NK92MI and primary NK cells primed by cytokine cocktails, the chemical priming method can be combined with established therapeutic NK cells that are currently under clinical evaluation for their antitumor efficacy. For instance, it would be interesting to examine whether 25KbPEI increases the antitumor activity of CAR-NKs in clinical trials of solid tumors as well as hematological cancers.[19]

Since cytolytic $CD8^+$ T cells exhibit antitumor activity in a perforin-dependent manner, it would also be an interesting question to ask whether 25KbPEI enhances the cytotoxic activity of these cells via a mechanism similar to that in NK cells. Immunotherapy of cancer is an emerging strategy. Chemical approaches to increasing the antitumor activity of immune cells would facilitate development of the next generation of immune cell products with potent clinical activity.

Contributors K-SP and K-HP conceived, designed, and supervised the study. SHC designed and performed all experiments, with assistance from JDP, E-SK, ML, D-KL, J-HC, HJJ and H-YJ. HJK designed the study and performed chemical synthesis, characterization and visualization. SHC and JDP performed animal experiments, with assistance from E-SK, M-WL. K-SP, K-HP, SHC and HJK wrote the manuscript. IK performed purification and expansion of human peripheral blood derived natural killer cells, with assistance from SHC and E-SK. K-SP is responsible for the overall content as the guarantor.

Funding This work was supported by Samsung Research Funding & Incubation Center of Samsung Electronics under Project Number SRFC_MA2102_06.

Competing interests None declared.

Patient consent for publication Not applicable.

Ethics approval This study involves human participants and was approved by institutional review board of CHA University (permit number: 1044308-202112-HR-097-02). Participants gave informed consent to participate in the study before taking part.

Provenance and peer review Not commissioned; externally peer reviewed.

Data availability statement All data relevant to the study are included in the article or uploaded as supplementary information.

ORCID iDs
Seung Hee Choi http://orcid.org/0000-0002-8736-7969
Joo Dong Park http://orcid.org/0000-0002-6131-878X
Eun-Su Ko http://orcid.org/0000-0002-0928-8069
Minwook Lee http://orcid.org/0000-0003-4986-9017

Keun-Hong Park http://orcid.org/0000-0002-0615-4313
Kyung-Soon Park http://orcid.org/0000-0002-0615-4313

REFERENCES

1 Li J, Fan C, Pei H, *et al*. Smart drug delivery nanocarriers with self-assembled DNA nanostructures. *Adv Mater* 2013;25:4386–96.
2 Zhang G, Zeng X, Li P. Nanomaterials in cancer-therapy drug delivery system. *J Biomed Nanotechnol* 2013;9:741–50.
3 Rudolph C, Ortiz A, Schillinger U, *et al*. Methodological optimization of polyethylenimine (PEI)-based gene delivery to the lungs of mice via aerosol application. *J Gene Med* 2005;7:59–66.
4 Boussif O, Lezoualc'h F, Zanta MA, *et al*. A versatile vector for gene and oligonucleotide transfer into cells in culture and in vivo: polyethylenimine. *Proc Natl Acad Sci U S A* 1995;92:7297–301.
5 Akinc A, Thomas M, Klibanov AM, *et al*. Exploring polyethylenimine-mediated DNA transfection and the proton sponge hypothesis. *J Gene Med* 2005;7:657–63.
6 Wojnilowicz M, Glab A, Bertucci A, *et al*. Super-resolution Imaging of proton sponge-triggered rupture of endosomes and cytosolic release of small interfering RNA. *ACS Nano* 2019;13:187–202.
7 Gao X, Yao L, Song Q, *et al*. The association of autophagy with polyethylenimine-induced cytotoxicity in nephritic and hepatic cell lines. *Biomaterials* 2011;32:8613–25.
8 Dolstra H, Roeven MWH, Spanholtz J, *et al*. Successful Transfer of Umbilical Cord Blood CD34^{+} Hematopoietic Stem and Progenitor-derived NK Cells in Older Acute Myeloid Leukemia Patients. *Clin Cancer Res* 2017;23:4107–18.
9 Siegler EL, Zhu Y, Wang P, *et al*. Off-the-shelf CAR-NK cells for cancer immunotherapy. *Cell Stem Cell* 2018;23:160–1.
10 Malaisé M, Rovira J, Renner P, *et al*. KLRG1+ NK cells protect T-bet-deficient mice from pulmonary metastatic colorectal carcinoma. *J Immunol* 2014;192:1954–61.
11 Putz EM, Mayfosh AJ, Kos K, *et al*. NK cell heparanase controls tumor invasion and immune surveillance. *J Clin Invest* 2017;127:2777–88.
12 Barry KC, Hsu J, Broz ML, *et al*. A natural killer-dendritic cell axis defines checkpoint therapy-responsive tumor microenvironments. *Nat Med* 2018;24:1178–91.
13 Liu E, Marin D, Banerjee P, *et al*. Use of CAR-transduced natural killer cells in CD19-positive lymphoid tumors. *N Engl J Med* 2020;382:545–53.
14 Ni J, Miller M, Stojanovic A, *et al*. Sustained effector function of IL-12/15/18-preactivated NK cells against established tumors. *J Exp Med* 2012;209:2351–65.
15 North J, Bakhsh I, Marden C, *et al*. Tumor-primed human natural killer cells lysE NK-resistant tumor targets: evidence of a two-stage process in resting NK cell activation. *J Immunol* 2007;178:85–94.
16 Cichocki F, Valamehr B, Bjordahl R, *et al*. GSK3 inhibition drives maturation of NK cells and enhances their antitumor activity. *Cancer Res* 2017;77:5664–75.
17 Kim K-S, Han J-H, Choi SH, *et al*. Cationic nanoparticle-mediated activation of natural killer cells for effective cancer immunotherapy. *ACS Appl Mater Interfaces* 2020;12:56731–40.
18 Choi YH, Lim EJ, Kim SW, *et al*. IL-27 enhances IL-15/IL-18-mediated activation of human natural killer cells. *J Immunother Cancer* 2019;7:168.
19 Liu S, Galat V, Galat Y, *et al*. NK cell-based cancer immunotherapy: from basic biology to clinical development. *J Hematol Oncol* 2021;14:7.
20 Wu Y, Tian Z, Wei H. Developmental and functional control of natural killer cells by cytokines. *Front Immunol* 2017;8:930.
21 Chaix J, Tessmer MS, Hoebe K, *et al*. Cutting edge: priming of NK cells by IL-18. *J Immunol* 2008;181:1627–31.
22 Huntington ND, Puthalakath H, Gunn P, *et al*. Interleukin 15-mediated survival of natural killer cells is determined by interactions among Bim, Noxa and Mcl-1. *Nat Immunol* 2007;8:856–63.
23 Caligiuri MA. Human natural killer cells. *Blood* 2008;112:461–9.
24 Björkström NK, Riese P, Heuts F, *et al*. Expression patterns of NKG2A, KIR, and CD57 define a process of CD56dim NK-cell differentiation uncoupled from NK-cell education. *Blood* 2010;116:3853–64.
25 Orange JS. Formation and function of the lytic NK-cell immunological synapse. *Nat Rev Immunol* 2008;8:713–25.
26 Brennan AJ, Law RHP, Conroy PJ, *et al*. Perforin proteostasis is regulated through its C2 domain: supra-physiological cell death mediated by T431D-perforin. *Cell Death Differ* 2018;25:1517–29.
27 Rah S-Y, Kwak J-Y, Chung Y-J, *et al*. ADP-ribose/TRPM2-mediated Ca2+ signaling is essential for cytolytic degranulation and antitumor activity of natural killer cells. *Sci Rep* 2015;5:9482.
28 Knowles H, Heizer JW, Li Y, *et al*. Transient receptor potential melastatin 2 (TRPM2) ion channel is required for innate immunity against Listeria monocytogenes. *Proc Natl Acad Sci U S A* 2011;108:11578–83.
29 Young JD, Hengartner H, Podack ER, *et al*. Purification and characterization of a cytolytic pore-forming protein from granules of cloned lymphocytes with natural killer activity. *Cell* 1986;44:849–59.
30 Pham CT, Ley TJ. Dipeptidyl peptidase I is required for the processing and activation of granzymes A and B in vivo. *Proc Natl Acad Sci U S A* 1999;96:8627–32.
31 Griffiths GM, Isaaz S. Granzymes A and B are targeted to the lytic granules of lymphocytes by the mannose-6-phosphate receptor. *J Cell Biol* 1993;120:885–96.
32 Glienke W, Esser R, Priesner C, *et al*. Advantages and applications of CAR-expressing natural killer cells. *Front Pharmacol* 2015;6:21.
33 Tettamanti S, Marin V, Pizzitola I, *et al*. Targeting of acute myeloid leukaemia by cytokine-induced killer cells redirected with a novel CD123-specific chimeric antigen receptor. *Br J Haematol* 2013;161:389–401.